Optics Letters

Reflection-induced linear polarization rotation and phase modulation between orthogonal waves for refractive index variation measurement

Ruey-Ching Twu* and Jhao-Sheng Wang

Department of Electro-Optical Engineering, Southern Taiwan University of Science and Technology, No. 1 Nan-Tai Street, Yungkang, Tainan 71005, Taiwan
*Corresponding author: rctwu@stust.edu.tw

Received 7 January 2016; revised 25 February 2016; accepted 10 March 2016; posted 10 March 2016 (Doc. ID 256998); published 1 April 2016

An optical phase interrogation is proposed to study reflection-induced linear polarization rotation in a common-path homodyne interferometer. This optical methodology can also be applied to the measurement of the refractive index variation of a liquid solution. The performance of the refractive index sensing structure is discussed theoretically, and the experimental results demonstrated a very good ability based on the proposed schemes. Compared with a conventional common-path heterodyne interferometer, the proposed homodyne interferometer with only a single channel reduced the usage of optic elements.

OCIS codes: (120.5050) Phase measurement; (120.5410) Polarimetry; (130.6010) Sensors.

http://dx.doi.org/10.1364/OL.41.001692

The propagation of light through an anisotropic material may change the polarization state. Among the optically anisotropic properties, the birefringence causes phase modulation between two orthogonal polarization planes; the chirality causes linear polarization rotation (LPR). The LPR in chiral media can be observed simply by utilizing a pair of polarizers. In a simple polarimeter, two polarizers are positioned so that no light passes through the combination. If an optical active sample is placed between these polarizers, light will pass again. By turning one of the polarizers to relocate the dark position, the amount of rotation introduced by the sample can be measured. To enhance the output signal contrast, the polarizers (Glan–Thompson) with a high polarization extinction ratio ($10^5:1$) are widely used for a fine angle resolution. The commercial polarimeters have been developed for application in the chemical, food, flavor, and pharmaceutical industries [1]. To increase the angle resolution for the measurement of LPR, phase measurements of the chiral-induced optical rotation have been demonstrated using common-path heterodyne interferometry [2–4]. Heterodyne light sources can be generated by using an electro-optic or acousto-optic modulator. Therein, the common-path arrangement based on electro-optic modulation [3] can reduce the alignment issues in comparison with the splitting path setup by using the acousto-optic modulator [2].

In past decades, reflection-type surface plasmon resonance (SPR) and total internal reflection sensors have been used in common-path polarimetric interferometers for measurement of the refractive index (RI) variation of liquid solutions [5–9]. In this Letter, a novel methodology based on reflection-induced LPR has been studied for the measurements of RI variation of liquid solutions. According to Fresnel's reflection principles [10], the reflectivity of the incident light is dependent on the polarization, angle of incidence, and relative RI between the solution and interface. In external reflection, there is a constant phase difference of π between the orthogonal polarizations (p-wave and s-wave) when the incident angle is less than Brewster's angle. Therefore, the intensity ratio between the orthogonal polarizations is dependent on the RI change of the tested solutions as well as the incident angle. The ratio variations will cause the azimuth angle to change. This behavior is similar to that of the chiral-induced LPR in the chiral solutions, and the changes of the azimuth angle are dependent on the activity and propagation length [2]. When the linearly polarized light passes through a half-wave plate (HWP) at a specific roll angle, the minor change of rotation angle will cause an obvious phase-delay change between the orthogonal polarizations. Then, the phase variation can be measured with the proposed common-path homodyne interferometer. A homemade Zn-indiffused lithium niobate phase modulator (ZIPM) is utilized to provide a sinusoidal phase modulation, and the measured phase information is extracted by using a LabVIEW-based platform [11]. The ZIPM is fabricated in an x-cut/z-propagating lithium niobate substrate. The waveguide-type phase modulator can provide a low applied voltage (<8 V) and stable phase operation. Compared with the measurement setup of a common-path heterodyne interferometer [3], the proposed homodyne interferometer with only a single channel reduced the usage of optic elements.

The measurement setup and refractive index sensor (RIS) are shown in Fig. 1. The illumination light from a He–Ne laser (632.8 nm) passes through a polarizer (PL) and half-wave plate. Next, the light with both orthogonal polarizations is coupled into the ZIPM through an objective lens (L1). Phase modulation

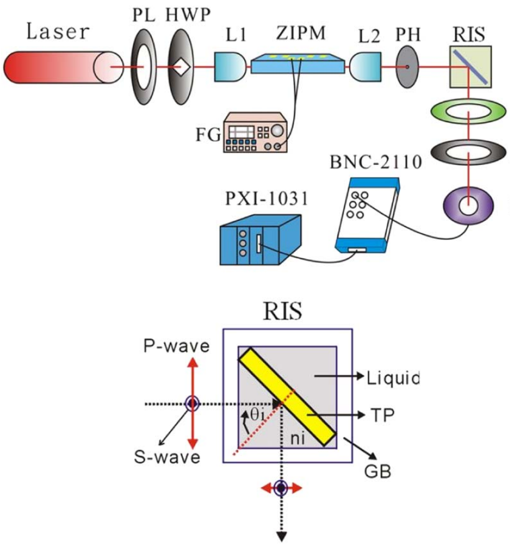

Fig. 1. Measurement setup and RIS structure.

light is generated by applying a sinusoidal voltage to the ZIPM from a function generator (FG). The output light from the ZIPM is then focused through another objective lens (L2). The scattering light is filtered out through a pinhole (PH). The sensing light propagates through the RIS, a near-half-wave plate (δWP), and an analyzer (AL) and then is received by a photodetector (PD). The converted electrical signal is sent to a signal acquisition box (BNC-2110) and analyzed in a LabVIEW platform (PXI-1031). The proposed RIS is fabricated using a cubic glass box (GB) with an embedded transparent plate (TP).

If the incident orthogonal polarizations (*p*- and *s*-wave) have the same intensity, the reflectivity of both polarizations is represented as the following [10]:

$$R_P = \left(\frac{n_i \cos\theta_t - n_{tp}\cos\theta_i}{n_i \cos\theta_t + n_{tp}\cos\theta_i}\right)^2, \tag{1}$$

$$R_S = \left(\frac{n_i \cos\theta_i - n_{ts}\cos\theta_t}{n_i \cos\theta_i + n_{ts}\cos\theta_t}\right)^2, \tag{2}$$

where R_p and R_s are the reflectance of *p*- and *s*-wave polarizations, respectively. n_{tp} and n_{ts} are the refractive indices of TP for *p*-and *s*-wave polarizations, respectively. The RI of the environmental liquid is defined as n_i. The incident and refracted angles are θ_i and θ_t, respectively. In cases where the incident angle is smaller than Brewster's angle, there is no additional angle-dependent phase delay between *p*- and *s*-wave polarizations. The effective azimuth angle is defined as

$$\beta = \tan^{-1}(-\sqrt{R_S/R_P}). \tag{3}$$

At the same incident angle, the azimuth angle is changed as well as the RI variation of the environmental liquid. In the proposed common-path homodyne interferometer, as shown in Fig. 1, a change in the azimuth angle ($\Delta\beta$) of the reflected light will make the phase delay change between two orthogonal polarizations after passing through the δWP. The phase delay can be written as [2]

$$\phi_{\mathrm{RI}} = \tan^{-1}\left[\tan\frac{1}{2}\delta(\cos 2(\Delta\beta+\alpha)+\sin 2(\Delta\beta+\alpha))\right] - \tan^{-1}\left[\tan\frac{1}{2}\delta(\cos 2(\Delta\beta+\alpha)-\sin 2(\Delta\beta+\alpha))\right], \tag{4}$$

where δ and α are the phase retardation and roll angle of δWP, respectively. The phase delay is not only dependent on $\Delta\beta$, but also is impacted by the phase retardation value of δWP. In common-path homodyne interferometry, the received interferometric intensity (I_{out}) with a sinusoidal phase modulation can be obtained as

$$I_{\mathrm{out}} = I_P + I_S + 2\sqrt{I_p \cdot I_S}\cdot\cos(\gamma\cdot\sin(2\pi f t)+\phi_{\mathrm{RI}}), \tag{5}$$

where I_p and I_s are the intensities of *p*- and *s*-wave polarizations, respectively. γ and f are the modulation depth and frequency of the applied voltage for phase modulation, respectively. γ is defined as

$$\gamma = \pi\cdot\frac{V_{\mathrm{ac}}}{V_\pi}, \tag{6}$$

where V_{ac} and V_π are the applied voltage and voltage for the phase change of π, respectively. The modulated interferometric signal is analyzed by a fast Fourier transform scheme. The spectrum, with different harmonic signals, can be used for calculating phase information during measurements. The components of the fundamental and second harmonic frequency (I_{1f} and I_{2f}) are represented by

$$I_{1f} = 4\sqrt{I_p\cdot I_S}\cdot\sin(\phi_{\mathrm{RI}})\cdot J_1(\gamma), \tag{7}$$

$$I_{2f} = 4\sqrt{I_p\cdot I_S}\cdot\cos(\phi_{\mathrm{RI}})\cdot J_2(\gamma), \tag{8}$$

where $J_1(\gamma)$ and $J_2(\gamma)$ are the first kind Bessel functions with different indices. According to Eqs. (7) and (8), the measured phase signal can be obtained as

$$\phi_{\mathrm{RI}} = \tan^{-1}\left(\frac{I_{1f}\cdot J_2(\gamma)}{I_{2f}\cdot J_1(\gamma)}\right). \tag{9}$$

The intensity ratio between Eqs. (7) and (8) eliminates the impact of varied intensity effects of I_p and I_s. This means that the phase signal is still stable even with the variations in I_p and I_s. It also can provide flexibility for the proposed new metrology schemes.

Figure 2 presents the calculated normalization values of transmittance and reflectance under the different angles of incidence for the three plates. The transmittance values of *s*- and *p*-wave polarizations are defined as T_s and T_p, respectively. In the simulations, the liquid solution is assumed to be 1.3330 refractive index units (RIU). Figure 2(a) gives the simulation results using an isotropic glass plate with an RI of 1.5. Figure 2(b) represents the simulation results using a birefringent $LiNbO_3$ (LN) with RIs ($n_{ts} = 2.2$ and $n_{tp} = 2.286$). Figure 2(c) represents the simulation results using a birefringent rutile (TiO_2) with RIs ($n_{ts} = 2.76$ and $n_{tp} = 2.49$). In the glass plate, the calculated results show that both *s*- and *p*-wave polarizations are the smallest due to the smaller RI difference between the glass and the surrounding liquid. The reflectance of a *p*-wave is near zero at the incident angle of 45 deg. This will make the interferometric signal undetectable in the common-path interferometer. Then, only the LN and TiO_2 plates are considered for further comparisons to be applied to the RI variation measurements of the liquid. At the incident angle of 45 deg, the normalized transmittance and reflectance as a function of the RI of the liquid for LN and TiO_2 plates are shown in Fig. 3.

The intensity ratios between *s*- and *p*-wave polarizations for both transmittance and reflectance can be further defined as the azimuth angle β, according to Eq. (3). The initial liquid

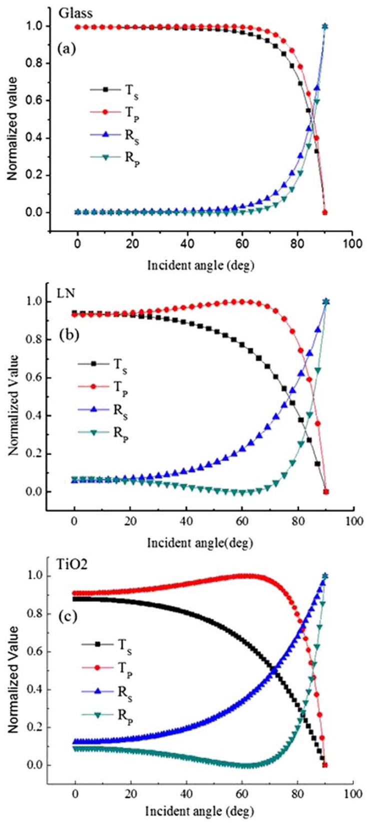

Fig. 2. Normalized transmittance and reflectance as a function of incident angle for three plates: (a) glass, (b) LN, and (c) TiO_2.

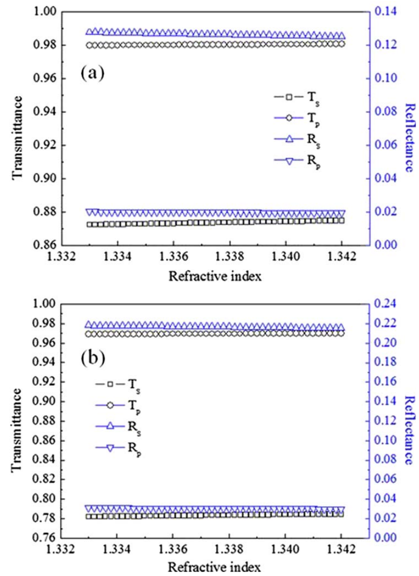

Fig. 3. Normalized transmittance and reflectance as a function of liquid refractive index for (a) LN and (b) TiO_2 plates.

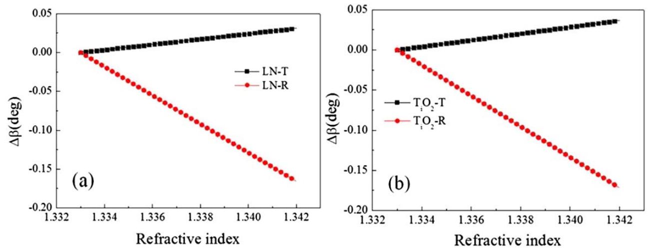

Fig. 4. Change of azimuth angle versus refractive index for (a) LN and (b) TiO_2 plates.

solution is assumed to be 1.3330 RIU; both changes of the azimuth angle ($\Delta\beta$) for the increased RIs are shown in Fig. 4.

The slopes of $d\Delta\beta/dn_i$ of the reflectance are around four times larger than those of the transmittance for both LN and TiO_2 plates. This means that the reflectance measurement will have more sensitivity than the transmittance one. The slopes of the reflectance curves are 18.44 and 19.11 for the LN and TiO_2 plates, respectively. The angle trace of LPR is negatively increased as an increase of RI. It is similar to a linearly polarized light propagating clockwise when passed through the sensing path. To experimentally demonstrate that the proposed new method can be applied for the measurement of RI variations in the liquid, various RIs can be adjusted by mixing with different weights of water and salt. A quasi-linear dependence of the RI change on the solution's concentration (wt. %) is possible [6]. The concentration, RI, and the corresponding $\Delta\beta$ for the LN and the TiO_2 plates are summarized in Table 1.

Since the price of an LN plate is cheaper than that of a TiO_2 one, the LN-based RIS at an incident angle of 45 deg was chosen for comparing the characteristics of phase measurement between the simulations and experiments. According to the parameters of Table 1 and Eq. (4), the simulated phase variation versus roll angle for various concentrations and the different values of δ of 178 and 179.9 deg are shown in Figs. 5(a) and 5(b), respectively. The results indicate that the sharper phase change can enhance the measurement's sensitivity when the value of δ is close to 180 deg. The behaviors are similar to the phase measurement performance in the SPR schemes [8]. However, an optimized thickness of gold film and precise initial angle are necessary for high sensitivity achievement in the SPR measurements. In the measurements, the δWP rotates clockwise. Therefore, the phase curves have a concentration-dependent shift toward the larger roll angle as the concentration increases.

According to the simulation results of Fig. 5, the greatest sensitivity angle occurs at the angle difference of 22.5 deg between the azimuth angle of the probe light and the fast axis of δWP. At the specific roll angle, Fig. 6 shows the simulated phase variation versus concentration for different values of δ. The dynamic phase change is increased with the increase of δ. To sustain enough of a linear relationship for phase variation and concentration change, a lower δ ($\delta = 178$ deg) would be better. If only considering the lower concentration measurements (<1.25%), the sensitivity can be enhanced greatly

Table 1. Refractive Indices and Azimuth Angle Changes of the LN and TiO_2 Plates for Different Concentrations of Salt Solution

Wt. %	0%	1.25%	2.5%	5%
n_i	1.3330	1.3353	1.3375	1.3420
LN($\Delta\beta$)	0	−0.04143	−0.08287	−0.16579
TiO_2($\Delta\beta$)	0	−0.04293	−0.08587	−0.17178

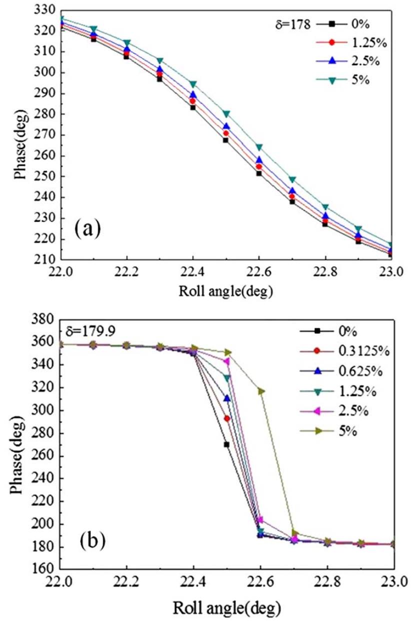

Fig. 5. Measured phase changes versus roll angle for various concentrations and the different values of δ: (a) $\delta = 178$ deg and (b) $\delta = 179.9$ deg.

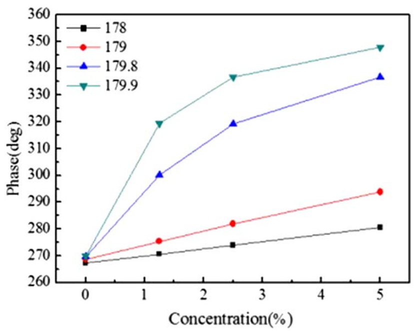

Fig. 6. Simulated phase variations for different concentrations of salt solutions at different values of δ.

when the values of δ are close to 180 deg. In the case ($\delta = 179.9$ deg), when the concentration is 1.25% with an increased RI of 2.25×10^{-3} RIU, the phase change is 50 deg. To evaluate the sensing performance, the measurement sensitivity is represented by the ratio of the phase difference versus the RI change [5]. The sensitivity of the RI measurement is around 2.22×10^4 (deg/RIU), which is comparable with the published papers utilizing SPR methods [5]. However, a simple structure with a bare LN plate is more flexible and attractive for the refraction index variation measurements.

In the real measurement setup, δWP is a near half-wave plate ($\delta \fallingdotseq 180$ deg). The plate is rotated through 45 deg with a step of 0.025 deg. Figure 7 shows the measured phase variation versus roll angle for various concentrations. As illustrated in Fig. 5(b), similar curves of phase variations and shifts are observed in different concentrations. To compare the experimental results with the simulations, pure water ($n_i = 1.3330$)

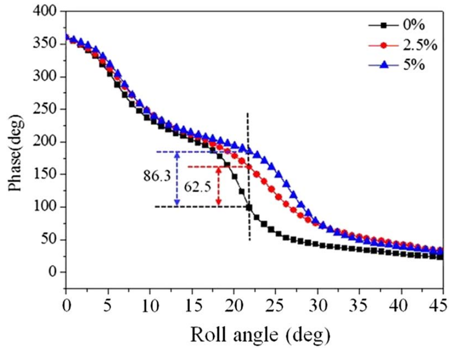

Fig. 7. Measured phase change versus roll angle for various concentrations.

is chosen as an initial base phase. At the most sensitive roll angle (marked by a vertical dashed line in Fig. 7), the values of the phase difference are 62.5 and 86.3 deg for concentrations of 2.5% ($n_i = 1.3375$) and 5% ($n_i = 1.3420$), respectively. Results are close to the simulation values ($\delta = 179.9$ deg), as shown in Fig. 6. In the RI range from 1.3330 to 1.3375 RIU, the measured phase change is 62.5 deg. Therefore, the sensitivity is around 1.39×10^4 (deg/RIU). The corresponding measurement resolution is defined by the ratio of measurement phase stability versus sensitivity. A phase measurement stability of 0.02 deg is achieved, thus indicating a measurement resolution of at least 1.43×10^{-6} RIU.

In conclusion, a principle of reflection-induced linear polarization rotation has been applied on the measurements of the RI variation of a liquid solution. The measurements are mainly based on the phase interrogation scheme; the proposed common-path and single-channel homodyne interferometer can provide a simpler measurement setup. Numerical simulations indicate that a RI variation measurement with a resolution of 1.43×10^{-6} RIU is achieved when the initial roll angle of the half-wave plate is optimized. This precision is verified by experiments, and the results show significant agreement with the simulation.

Funding. Ministry of Science and Technology, Taiwan (MOST) (MOST 104-2221-E-218-027).

REFERENCES

1. Rudolph Research Analytical, http://rudolphresearch.com.
2. C. M. Wu and Y. C. Tsai, Sens. Actuators B **120**, 324 (2006).
3. J. Y. Lin and D. C. Su, Opt. Commun. **256**, 337 (2005).
4. J. Y. Lin, K. Huang, and J. H. Chen, Appl. Opt. **46**, 5944 (2007).
5. Y. L. Lo, C. H. Chuang, and Z. W. Lin, Sens. Actuators B **158**, 400 (2011).
6. J. Y. Lee and S. K. Tsai, Opt. Commun. **284**, 925 (2011).
7. Y. H. Huang, H. P. Ho, S. Y. Wu, S. K. Kong, W. W. Wong, and P. Shum, Opt. Lett. **36**, 4092 (2011).
8. S. Patskovsky, M. Meunier, and A. V. Kabashin, Opt. Express **15**, 12523 (2007).
9. M. Maisonneuve, I.-H. Song, S. Patskovsky, and M. Meunier, Opt. Express **19**, 7410 (2011).
10. C. A. Bennett, *Principles of Physical Optics* (Wiley, 2008).
11. R. C. Twu, H. Y. Hong, and H. H. Lee, Opt. Lett. **33**, 2530 (2008).